Ultrasonics Sonochemistry 118 (2025) 107364

Contents lists available at ScienceDirect

Ultrasonics Sonochemistry

journal homepage: www.elsevier.com/locate/ultson

Ultrasound-Assisted extraction and purification of polysaccharides from *Boschniakia rossica*: Structural Characterization and antioxidant potential

Minghui Yang [a,b,1], Xingfan Li [a,b,1], Xinyi Du [a,b], Falin Li [a,b], Tianqi Wang [a,b], Yanyan Gao [a,b], Jia Liu [c], Xiongfei Luo [a,b], Xiaorui Guo [a,b,*], Zhonghua Tang [a,b,*]

[a] College of Chemistry, Chemical Engineering and Resource Utilization, Northeast Forestry University, Harbin 150040, China
[b] Key Laboratory of Forest Plant Ecology, Ministry of Education, Northeast Forestry University, Harbin 150040, China
[c] Key Laboratory of Soybean Molecular Design Breeding, Northeast Institute of Geography and Agroecology, Chinese Academy of Sciences, Harbin 150040, China

ARTICLE INFO

Keywords:
Ultrasonic-assisted enzyme extraction
Polysaccharides
Structural analysis
Biological activity

ABSTRACT

Modern pharmacological investigations have shown that polysaccharides extracted from *Boschniakia rossica* showcase a range of biological effects. This study identified 260 primary metabolites, with carbohydrate compounds and their derivatives accounting for 80 types. We employed ultrasonic-assisted enzyme extraction (UAEE) to optimize extraction parameters, achieving a crude polysaccharide yield of 13.67%, which is 1.52 times and 1.17 times higher than ultrasonic extraction (UAE) and enzyme extraction (EAE). Additionally, we isolated four distinct purified polysaccharides (BRPS-0, BRPS-1, BRPS-2, BRPS-3), with relative molecular weights of 1569, 2815, and 4572, while BRPS-3 displayed structural complexity. The scanning electron microscope (SEM) revealed that BRPS-0 exhibited distinct crystalline particles, while BRPS-3 displayed an ordered crystal structure. Notably, BRPS-0 demonstrated relatively stable antioxidant activity due to its low molecular weight, high phenolic and sugar content, crystalline microstructure, and abundant α- and β-pyranose configurations, including galacturonic acid, glucose, galactose, and arabinose. This research provides a foundational theory for the comprehensive use of *Boschniakia rossica* resources and supports its implementation in modern medicine and functional foods.

1. Introduction

Boschniakia rossica Fedtsch. et Flerov, is a perennial herbaceous plant belonging to the Orobanchaceae family. It attaches to the roots of genus *Alnus* species (*Betulaceae*) and is widely distributed in eastern regions and western parts of North America. The biological activity of *Boschniakia rossica* is primarily attributed to the diversity of its chemical constituents, which mainly include polysaccharides, cycloartanes, and phenylpropanoids [1]. Modern pharmacological research has focused on the study of polysaccharide activity in *Boschniakia rossica*, identifying two main types of glycosides present: phenylpropanoid glycosides and syringin, which exhibit significant anti-inflammatory properties [2]. Additionally, it demonstrates various biological activities, including free radical scavenging [3], anti-aging [4], anti-tumor, anti-cancer [5], as well as hepatoprotective and immune-enhancing effects. Plant-derived polysaccharides have gained attention in biomedicine for their low toxicity and anti-tumor activity, as they enhance innate immunity by stimulating macrophages and regulating the complement system while also being used alongside chemotherapy drugs for cancer treatment [6].

As research on the polysaccharides of *Boschniakia rossica* deepens, optimizing extraction methods has become particularly important. Traditional extraction methods often suffer from low efficiency and long processing times, making them unsuitable for meeting modern production demands. Therefore, the exploration of efficient, rapid, and environmentally friendly extraction technologies has become a major focus of current research [7–10]. Among the various techniques, ultrasonic extraction (UAE) and enzyme extraction (EAE) have gained significant attention due to their respective advantages. UAE leverages the cavitation effect of high-frequency vibrations to disrupt plant cell walls, facilitating the release of active components and enhancing extraction efficiency [11–13]. In contrast, EAE selectively degrades cell walls using specific enzymes, reducing physical resistance and preserving biological activity [14,15]. Combining the advantages of both methods, ultrasound-assisted enzyme extraction (UAEE) employs high-frequency

* Corresponding authors.
E-mail addresses: xruiguo@nefu.edu.cn (X. Guo), tangzh@nefu.edu.cn (Z. Tang).
[1] These authors contributed equally to this work.

https://doi.org/10.1016/j.ultsonch.2025.107364
Received 26 February 2025; Received in revised form 11 April 2025; Accepted 20 April 2025
Available online 21 April 2025

ultrasound and selective enzyme degradation to generate intense shock waves that effectively disrupt cell walls, increase solvent permeability, and accelerate the release of active components. UAEE significantly improves extraction efficiency, shortens extraction time, and yields high-purity polysaccharides while better protecting heat-sensitive components. This environmentally friendly process maintains the biological activity of the extracts under mild conditions, reducing the risk of component degradation and showing great promise as a modern extraction technology [16–18]. For instance, a total sugar content of 75.65 % was achieved from lychee pericarp polysaccharides using UAEE, demonstrating strong antioxidant and reducing abilities [19]. While research has predominantly focused on *Cistanche deserticola*, a species known for its effects and potential therapeutic applications, research on *Boschniakia rossica* has lagged despite its promising medicinal properties [20,21].

Building on previous research, three polysaccharides (BRR-W1, BRR-WA1, and BRR-WA2) were separated from the water extract of *Boschniakia rossica* [22], this study further employs UAEE combined with response surface methodology (RSM) to obtain higher-yield polysaccharides (BRPS) with superior antioxidant activity. Four purified components (BRPS-0, BRPS-1, BRPS-2, and BRPS-3) were successfully separated using a DEAE-52 cellulose column, and their relative molecular weights, microscopic morphologies, functional groups, and antioxidant activities were determined, revealing that BRPS-0 exhibited stable antioxidant activity. Furthermore, through monosaccharide composition analysis and nuclear magnetic resonance (NMR), the structural characteristics of BRPS-0 were preliminarily explored, leading to an in-depth discussion on how its molecular weight, crystal structure, conformation, and monosaccharide composition influence its antioxidant bioactivity. This research addresses aspects not thoroughly covered in previous studies, optimizes the preparation and application of *Boschniakia rossica* polysaccharides, fills research gaps, and supports the modernization of traditional Chinese medicine while providing a theoretical foundation for the development of its resources and future drug applications.

2. Materials and methods

2.1. Materials and reagents

The dried fleshy stems and roots of *Boschniakia rossica* were provided by the Tuqiang Forestry Bureau in the Greater Khingan Range, Heilongjiang Province, China. The stems and roots were pulverized using a grinder and passed through an 80-mesh sieve. The resulting powder is stored in a sealed container at room temperature for future use.

2.2. Primary metabolite extraction and detection

The analysis of primary metabolites followed a previously established protocol [23]. In brief, 90 mg of dried stem tissue from *Boschniakia rossica* was combined with 560 μL of the internal standard 2-chloro-L-phenylalanine (methanol solution, 0.3 mg/mL) and subjected to ultrasonication for 30 min. Subsequently, 300 μL of chloroform and 600 μL of deionized water were added, and a second round of ultrasonication was conducted for another 30 min. The supernatant was collected via low-temperature centrifugation, dried, and then reconstituted in 400 μL of methoxyamine hydrochloride in pyridine. After allowing oxime formation at 37 °C for 90 min in a shaking incubator, BSTFA and TMCS were introduced for derivatization prior to GC–MS (Agilent 7890-5977B, USA) analysis. For further details regarding sample preparation and equipment parameters, please consult the supplementary information **(Text S1)**.

2.3. Evaluation of polysaccharide concentration

A phenol–sulfuric acid assay was used to measure the crude polysaccharide content in *Boschniakia rossica*. One milligram of glucose standard was dissolved to 10 mL (100 μg/mL). Then, 0, 1, 2, 4, 8, and 10 mL of this stock were each diluted to 10 mL to create a series of glucose standards. For each standard, 0.2 mL was mixed with 0.1 mL of 6 % phenol and incubated for 5 min. Then 0.4 mL of concentrated sulfuric acid was added, thoroughly mixed, and left to react for 30 min. Use the zero μg/mL glucose solution as a blank to establish a standard curve correlating glucose concentration (x-axis) with absorbance (y-axis). For samples, 0.1 mL was diluted to 7 mL, and 0.2 mL of this solution was used in the assay. The absorbance was then applied to the standard curve equation to determine polysaccharide yield.

2.4. Orthogonal experiment design for composite enzyme formulation

Using the amounts of cellulase (A), pectinase (B), and papain (C) as independent variables, an orthogonal experiment design was carried out to examine the impact of the composite enzyme formulation on BRPS. The factor levels are presented in supplementary information **(Table S1)**.

2.5. Preparation of crude polysaccharide

One gram of *Boschniakia rossica* powder was weighed into a 50 mL centrifuge tube, and 25 mL of ethanol (60 %-100 %) is added to achieve a 1:25 (g/mL) solid-to-liquid ratio, forming the rossica solution. Under optimal enzymatic conditions, 0.05 g of cellulase, 0.04 g of pectinase, and 0.04 g of papain were then introduced. UAEE was conducted at 300–500 w, 40–80 °C, and for 0.5–3 h. After extraction, the enzymes were inactivated by heating in a water bath for 15 min, followed by cooling and centrifugation to obtain the supernatant.

2.6. One-way experiment

The extraction experiment focused on a single factor under the following specific conditions, with the experimental design presented in **(**Table 1**)**.

2.7. Response surface optimization

Drawing from the findings of the single-factor experiments, the levels of various factors were established **(Table S2)**. The Box-Bohken (B-B) design was utilized for optimization. The equation expresses the model: $Y = \beta_0 + \sum \beta_i X_i + \sum \beta_{ii} X_i^2 + \sum \beta_{ij} X_i X_j$, where Y represents the predicted BRPS, X_i and X_j denote the levels of independent variables, and β_i, β_{ii}, and β_{ij} are the coefficients for the model's intercept, linear, quadratic, and interaction terms.

2.8. Comparison of diverse extraction strategies

The results of three extraction procedures (UAEE, UAE, ENE) on the yield of polysaccharides were compared. The supplementary document (Text S2) provides a detailed description of the methods.

Table 1
Design of experiments with single variables.

Single factor	Concentration (%)	Time (h)	Temperature (°C)	Power (w)
Concentration	60, 70, 80, 90, 100	1	50	500
Time	70	0.5, 1, 1.5, 2, 3	50	500
Temperature	70	1	40, 50, 60, 70, 80	500
Power	70	1	50	300, 350, 400, 450, 500

2.9. Isolation and refinement of polysaccharides

2.9.1. Deproteinization and decolorization

The crude polysaccharide powder obtained from freeze-drying under optimal conditions was dissolved in distilled water and mixed with Sevag reagent at a 4:1 vol ratio. The mixture was shaken in a constant-temperature incubator for 30 min, then centrifuged at 8000 rpm for 15 min to collect the supernatant. This process was repeated three times. Next, an equal volume of 30 % hydrogen peroxide was added, and decolorization was carried out at 60 °C for 4 h. Finally, the deproteinized and decolorized polysaccharide solution was preserved by vacuum freeze-drying.

2.9.2. Separation and purification of BRPS

500 mg of deproteinized and decolorized polysaccharides from *Boschniakia rossica* (BRPS) were dissolved in 10 mL of distilled water. The resulting polysaccharide solution was then slowly introduced into a DEAE-52 column, where it was eluted and collected using 400 mL of deionized water and sodium chloride solutions at concentrations of 0.1, 0.3, and 0.5 mol/L. Each fraction was collected in 10 mL increments. The absorbance of each fraction was monitored via the phenol–sulfuric acid method, enabling the plotting of the elution curve. Fractions containing polysaccharides were combined, concentrated, and dialyzed (2000 Da) to remove small molecules, such as sodium chloride. Finally, the resulting solution is freeze-dried to obtain the purified polysaccharides.

2.10. The physicochemical characteristics associated with polysaccharides

The Coomassie Brilliant Blue method was employed to determine the protein content of the purified components. The total reducing sugars were quantified using the DNS method. The Folin-Ciocalteu method was utilized to assess the total phenolic content, while the aluminum-nitrite color development method was used to measure the total flavonoids. Detailed methodologies can be found in the supplementary file **(Text S3)**.

2.11. Characterization of structural properties

2.11.1. Infrared spectral analysis

10 Mg of BRPS-0, BRPS-1, BRPS-2, and BRPS-3 were mixed with potassium bromide as a dispersant and pressed into tablets. These tablets were scanned using a Fourier transform infrared spectrometer (Nicolet Summit, Thermo Fisher, USA) in the wavenumber range of 4000–500 cm^{-1}.

2.11.2. Relative molecular weight determination

The polysaccharide was dissolved in 0.1 % NaN_3 to a 5 mg/mL concentration and filtered using a 0.45 μm membrane. Analysis was performed using a high-performance liquid chromatograph (Shimadzu LC20, Japan) with a differential refractive index detector (RID-20, Shimadzu, Japan). The gel permeation chromatography column was TSKgel GMPWXL (TOSOH, 300 mm × 7.8 mm, Japan). Refer to the Appendix for the elution procedure parameters **(Text S4)**.

2.11.3. Assessment of the monosaccharide profile

According to the method by Wang et al. [24], the monosaccharide composition of BRPS-0 was analyzed with slight modifications. The standard monosaccharides were prepared as a 1 mg/mL solution and mixed with 1 mL of a 0.5 mol/L PMP methanol solution. The mixture was reacted at 70 °C for 2.5 h. After cooling the sample to room temperature, 1 mL of 0.2 mol/L hydrochloric acid and 1 mL of dichloromethane were added for multiple liquid–liquid extractions. The supernatant was collected and filtered through a 0.45 μm organic membrane to remove larger particulate impurities. The sample was hydrolyzed using trifluoroacetic acid (TFA, 4 mol/L) under nitrogen protection at 110 °C for 5 h. The derivatization was performed in the same manner as the standard monosaccharides [25]. Detection was carried out using a WUFENG LC-100 liquid chromatograph (Shanghai). For specific elution program parameters, see the Appendix **(Text S5)**.

2.11.4. SEM examination

Scanning electron microscopy (SEM) was employed to examine the micromorphology of polysaccharides from *Boschniakia rossica*. In relation to the Liu et al. [26], the purified and dried polysaccharide samples (BRPS-0, BRPS-1, BRPS-2, and BRPS-3) were placed on mica sheets and allowed to dry before being gold-coated. Observations and image acquisitions were conducted using a field emission scanning electron microscope (JSM-7500F, Japan) at magnifications of 500x and 10,000x, respectively.

2.12. Antioxidant activity assessment

Using 2,2-Diphenyl-1-picrylhydrazyl (DPPH) and 2,2′-Azino-bis(3-ethylbenzothiazoline-6-sulfonic acid (ABTS) radical scavenging assays, the extracts were reacted with DPPH and ABTS working solutions at different concentrations (100, 125, 250, 500, and 1000 μg/mL) to determine their scavenging rates. The DPPH scavenging rate was calculated by measuring the absorbance at 517 nm, while the ABTS scavenging rate was measured at 734 nm. The ferric − reducing antioxidant potential (FRAP) was assessed by reacting the extracts with the FRAP reagent and measuring the absorbance at 593 nm. For specific experimental details, please refer to Appendix **(Text S6)**.

2.13. Statistical analysis

Mean values were compared using a 95 % confidence interval Tukey test and one-way ANOVA, performed with IBM SPSS Statistics 26.0. The extraction parameters were optimized using Design-Expert DX-8 software. All measurements were taken in triplicate and reported as mean ± standard deviation. Metabolic pathways were constructed based on the Kyoto Encyclopedia of Genes and Genomes (KEGG) database (http://www.genome.jp/kegg/).

3. Results and discussion

3.1. Metabolite analysis of Boschniakia rossica

260 primary metabolites were identified, including 80 carbohydrates and derivatives, 51 organic acids, 43 alcohols, and other classes **(**Fig. 1a**)**. Carbohydrates were predominant, with 80 compounds mapped to the KEGG database, revealing 42 compounds linked to 11 metabolic pathways **(**Fig. 1b**)**. It is essential to highlight that pathways such as starch and sucrose metabolism, amino sugars, nucleotide sugar metabolism, galactose metabolism, pentose and glucuronate interconversion, fructose and mannose metabolism, the pentose phosphate pathway, glycerolipid metabolism, and ascorbate and alternate metabolism were significantly enriched ($p < 0.05$). These enriched pathways form a complex network underlying carbohydrate metabolism in *Boschniakia rossica*, indicating the use of diverse carbohydrate substrates for energy production, biosynthesis, and environmental stress response [27]. Specifically, the starch and sucrose metabolism pathway generates glucose, serving as the primary energy source for growth and development [28,29]. Amino sugars and nucleotide sugar metabolism are involved in synthesizing cell walls and genetic material [30]. The pentose phosphate pathway provides the precursors and reduces the power necessary for biosynthesis [31]. Metabolites of ascorbic acid and aldaric acid are key components of plant osmoprotectants [32], enhancing the plant's antioxidant defense system by directly scavenging toxic reactive oxygen species (ROS) and protecting fundamental antioxidant enzymes [33]. Therefore, these enriched carbohydrate

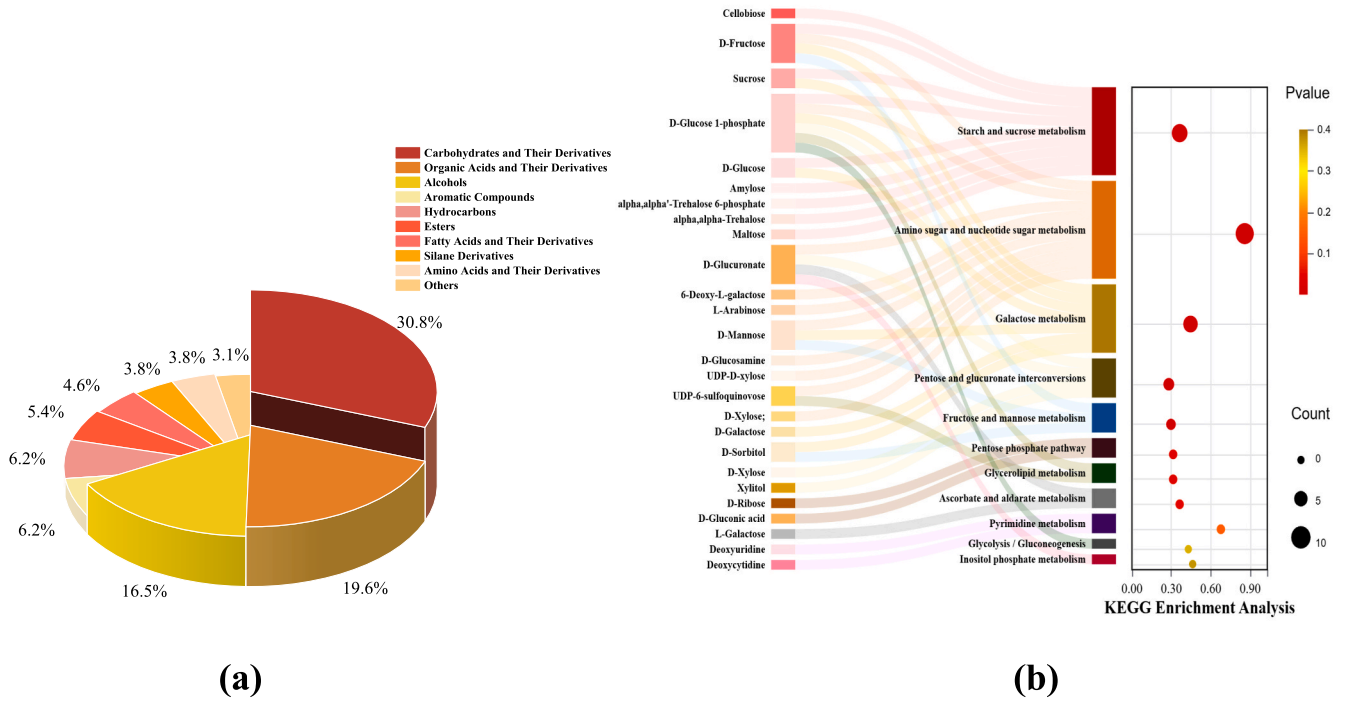

Fig. 1. The metabolite profile of *Boschniakia rossica*. (a) Relative abundance distribution across different compound classes. (b) KEGG pathway enrichment. Larger circles represent greater quantities of sugars enriched in the pathway. Circles with colors closer to red indicate a more significant level of enrichment. (For interpretation of the references to color in this figure legend, the reader is referred to the web version of this article.)

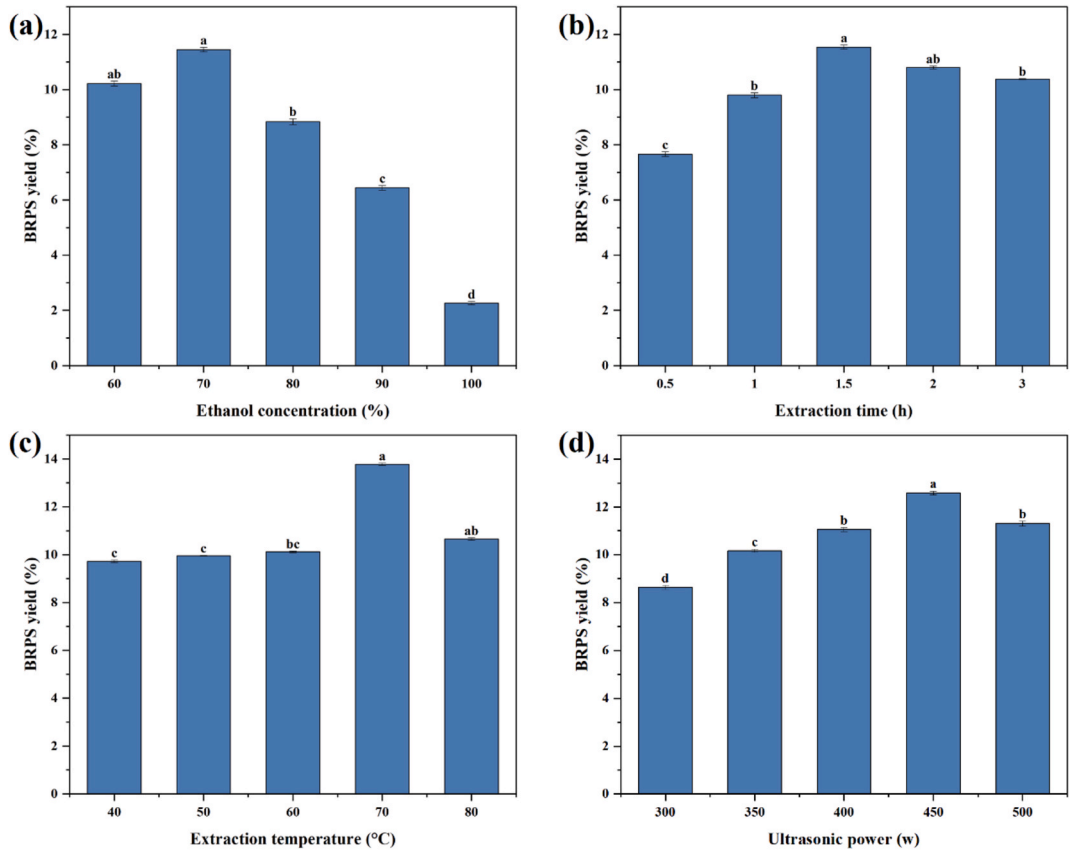

Fig. 2. The extraction yield was influenced by various factors, including different ethanol concentrations (a), extraction times (b), extraction temperatures (c), and ultrasonic power (d). Different letters (a, b, c, d) indicate significant differences, while the same letters signify no significant difference at ($p < 0.05$).

metabolic pathways are essential for *Boschniakia rossica*'s survival and environmental adaptation.

3.2. Orthogonal experiment for composite enzyme formulation

As indicated in the supplementary information (**Table S3**), the factors influencing the yield of crude polysaccharides from *Boschniakia rossica* are ranked as follows: papain > cellulase > pectinase. The optimal formulation is $A_3B_2C_2$, with cellulase at 5 %, pectinase at 4 %, and papain at 4 %.

3.3. Analysis of one-way experiment

3.3.1. Ethanol concentration ratio's influence on BRPS yield

Polysaccharide yield increases with rising ethanol concentration, peaking at 11.45 % ± 0.04 % at 70 % (Fig. 2a). Above 70 %, yield decreases due to reduced water content, weakened hydrogen bonding with polysaccharide hydroxyl groups, and subsequent precipitation. At optimal concentrations, ethanol effectively disrupts polysaccharide chain interactions, boosting solubility and extraction. Additionally, ethanol competes with polysaccharide functional groups for hydrogen bonding, further influencing yield [34].

3.3.2. Impact of extraction time on BRPS yield

As depicted in (Fig. 2b), the yield of BRPS initially rises and then falls with increased extraction time, attaining its peak value at 1.5 h. Insufficient extraction time may limit polysaccharide release, while moderate extension enhances solubility and promotes cell wall disruption via cavitation, maximizing yield [35]. Beyond 2–3 h, overexposure to ultrasound raises local temperatures and generates free radicals, causing polysaccharide degradation and lowering yield, leading to thermal and oxidative degradation of polysaccharides and reducing the content of polysaccharides [36].

3.3.3. Role of extraction temperature in BRPS yield

Between 40–60 °C (Fig. 2c), polysaccharides extraction efficiency is relatively low due to limited hydrogen bonds disruption, which maintains strong interactions with the solvent, preventing significant increases in solubility and extraction efficiency. Additionally, the increase in molecular kinetic energy is restricted, resulting in low diffusion rates that slow the release of polysaccharides from plant cells. Furthermore, insufficient cavitation effects during ultrasonic extraction further hinder efficiency. At 70 °C, hydrogen bond disruption increases, enhancing molecular kinetic energy and diffusion rates. More effective cavitation bubble formation generates stronger shock waves that disrupt cell walls, significantly improving extraction yield. Reduced surface tension also allows better solvent penetration into plant cells, enhancing polysaccharide release [37]. Above 70 °C, extraction yield declines rapidly, primarily due to thermal degradation of polysaccharide chains and free radical generation, which cause structural damage. In addition, the increased temperature raises the solvent's vapor pressure, affecting the shear force of ultrasound and reducing extraction efficiency [38].

3.3.4. BRPS yield was affected by ultrasonic power

From 300 w to 450 w (Fig. 2d), the yield of BRPS increases significantly due to enhanced cavitation, thermal effects, and mechanical effects, which work together to disrupt cell walls, improve solvent permeability, and accelerate the release of active components. The cavitation effect, by forming and collapsing tiny bubbles, generates strong local pressure and temperature changes that effectively break down cell wall structures, facilitating the release of polysaccharides into the solvent. Meanwhile, the thermal effect raises solvent temperature, increasing molecular motion and promoting dissolution and extraction. Additionally, ultrasonic vibrations enhance solvent contact with cell walls, further improving extraction efficiency [39]. However, beyond 450 w, yield drops because excessive ultrasound power increases temperature, causing thermal degradation or reduced molecular weight, and strong mechanical effects can damage the BRPS structure, diminishing its bioactivity [40].

3.4. Response surface methodology analysis of experimental design

3.4.1. BBD-RSM model

The extraction conditions were further optimized through a combination of BBD and RSM, as shown by the results of 29 experiments in (**Table S4**). A multiple regression analysis yielded the following fitting equation: $BRPS = 13.46 - 0.18A + 0.20B + 1.20C + 0.50D + 0.22AB + 0.13AC - 0.015AD - 0.042BC + 0.15BD - 0.16CD - 0.91A^2 - 0.84B^2 - 2.04C^2 - 2.65D^2$. The analysis of variance (ANOVA) results shows a high overall significance ($F = 83.20$, $p < 0.0001$), and an insignificant lack of fit ($p = 0.0728$), indicating a good model fit (Table 2). Factors C and D, as well as quadratic terms A^2, B^2, C^2, and D^2, have extreme significance ($p < 0.0001$). The interaction term AB ($p < 0.05$) is significant, suggesting ethanol concentration and extraction time have a considerable interactive effect on BRPS yield [41].

3.4.2. Response surface interaction analysis

The 3D response surface plot (Fig. 3a-f) visually reveals how four factors affect BRPS yield, with steeper gradients indicating stronger interactions and elliptical contours (**Fig. S1**) pointing to significant two-factor effects [42]. BRPS generally rises with extraction time and temperature, but reaches its peak at optimal ethanol concentrations and ultrasonic power. Beyond these thresholds, yield may drop due to solvent polarity shifts or component degradation. Notably, ethanol concentration and extraction time exert the greatest influence (Fig. 3a), while interactions between ethanol concentration and ultrasonic power, as well as extraction time and extraction temperature, are not statistically significant, consistent with the ANOVA results [43].

3.4.3. Optimization and validation results of the model

The model identified 80 % ethanol, 97.42 min, 73.20 °C, and 454.40 w as optimal conditions, predicting a BRPS yield of 12.64 %. For practicality, these were adjusted to 80 % ethanol, 100 min, 73 °C, and 450 w. Under these revised conditions, three parallel trials averaged a BRPS yield of 13.67 %.

Table 2
ANOVA for reponse surface quadratic model.

Source	Sum of Squares	df	Mean square	F Value	Prob > F
Model	83.2	14	5.94	37.03	<0.0001***
A-Ethanol concentration (%)	0.40	1	0.40	2.18	0.0061**
B-Extraction time (h)	0.48	1	0.48	3.38	0.0035**
C-Extraction temperature (°C)	17.21	1	17.21	98.14	<0.0001***
D-Ultrasonic power (w)	3.02	1	3.02	13.65	<0.0001***
AB	0.19	1	0.19	1.35	0.0445*
AC	0.070	1	0.070	0.5	0.2002
AD	0.0009	1	0.0009	0.21	0.8812
BC	0.0007	1	0.0007	0.051	0.6729
BD	0.087	1	0.087	0.62	0.1567
CD	0.11	1	0.11	1.28	0.1214
A^2	5.42	1	5.42	45.22	<0.0001***
B^2	4.56	1	4.56	35.63	<0.0001***
C^2	27.01	1	27.01	165.43	<0.0001***
D^2	45.45	1	45.45	296.42	<0.0001***
Residual	0.54	14	0.039		
Lack of Fit	0.50	10	0.050	4.77	0.0728
Pure Error	0.042	4	0.011		
Cor total	83.74	28			

* Denotes a significant difference with $p < 0.05$.
** Denotes a significant difference with $p < 0.01$.
*** Denotes a significant difference with $p < 0.001$.

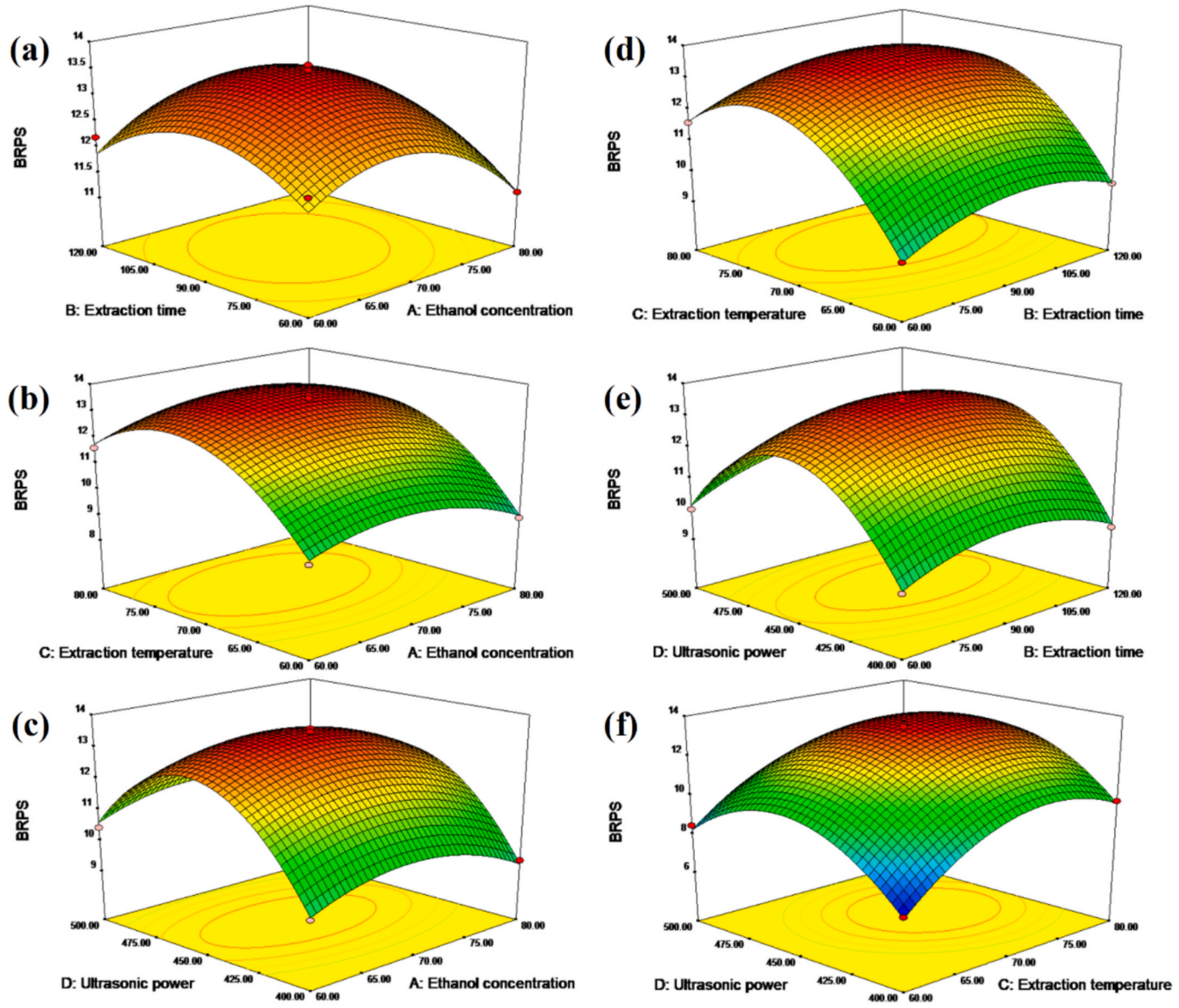

Fig. 3. 3D Response surface plots and for interaction between various factors on the yield of BRPS.

3.4.4. *Comparison with other extraction methods*

UAEE provides the highest BRPS yield, reaching 1.52 times that of UAE and 1.17 times that of EAE (Fig. 4). Scanning electron microscopy shows a gradient in the destruction of the cell wall of *Boschniakia rossica* across UAE, EAE, and UAEE, from partial fragmentation with ultrasound to targeted enzyme degradation and comprehensive disintegration with the combined treatment (**Fig. S2**). After UAEE, the residues treated with ultrasonic-assisted enzyme extraction (UAEE) exhibit the most significant cellular damage and exposure of internal structures, with surfaces covered by numerous widely distributed pores and cracks and previously intact tissues visibly peeled or decomposed into sheet-like or porous network fragments. The cavitation effect induced by ultrasound enhances the mechanical disruption of cell walls, enabling enzymes to penetrate deeper into target substrates, such as cellulose, pectin, and proteins, thereby achieving efficient degradation. This synergistic effect of "external force and enzymatic hydrolysis" significantly improves substrate permeability and facilitates thorough cell wall disruption in a relatively short time [44]. In contrast, EAE shows specific destruction of the cell wall, leading to noticeable collapse and peeling that results in a porous appearance due to enzyme degradation, but its ability to break down hard cell walls primarily depends on enzyme reaction efficiency [45]. Meanwhile, UAE retains larger block-like structures with depressions, indicating limited ultrasound cavitation effects on exposing internal components. Additionally, UAEE shows higher antioxidant activity, with better DPPH and ABTS scavenging rates and iron ion reduction compared to EAE and UAE (**Fig. S3**).

3.5. *Isolation and purification of BRPS*

Four distinct elution peaks were obtained, which were subsequently collected, concentrated, dialyzed, and freeze-dried, and were designated as BRPS-0, BRPS-1, BRPS-2, and BRPS-3 (Fig. 5).

3.6. *Analysis of the physicochemical properties of polysaccharides*

The total sugar contents in the BRPS crude extract, BRPS-0, −1, −2, and −3 were 13.67 %, 62.23 %, 26.99 %, 56.44 %, and 13.57 %, respectively (Fig. 6a). Purification significantly raised total and reducing sugar levels, indicating effective enrichment (Fig. 6a-b). Meanwhile, total polyphenols and proteins dropped below 1 % (Fig. 6c-d), suggesting removal or degradation during purification. Despite this reduction, a small quantity of flavonoids was still detected (Fig. 6e),

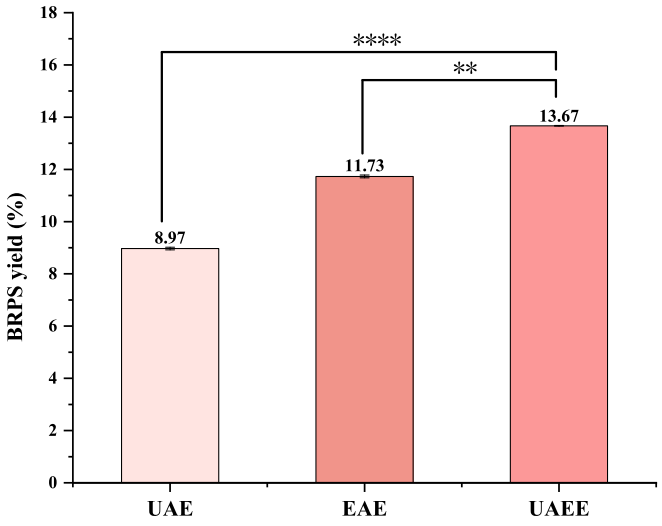

Fig. 4. In comparing various extraction methods. **** denotes a significant difference between the UAEE and UAE methods at the 0.0001 level, while ** indicates a significant difference between the UAEE and EAE methods at the 0.05 level.

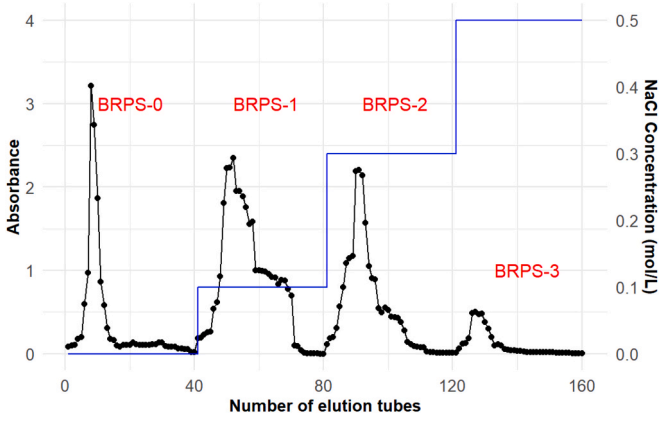

Fig. 5. DEAE-52 elution curve.

suggesting that certain bioactive compounds were preserved throughout the purification process. Overall, these findings highlight the selective enrichment of sugar components, which may have implications for the bioactivity and nutritional value of the purified fractions. Further investigation into the impacts of these compositional changes on antioxidant activity and other functional properties is warranted.

3.7. Characterization of BRPS

3.7.1. Assessment of relative molecular weight (Mn and Mw)

Using gel permeation chromatography (GPC), the relative molecular weights of BRPS-0, BRPS-1, BRPS-2, and BRPS-3 were determined (Table 3). BRPS-0, BRPS-1, and BRPS-2 each displayed a single, symmetrical peak, indicating homogeneous polysaccharides with relative molecular weights of 1569, 2815, and 4572, respectively (**Fig. S4**). In contrast, BRPS-3 exhibited two peaks, reflecting its structural complexity: one peak at 4871 and another at 961.

3.7.2. SEM observation of BRPS

Visual observations reveal that the freeze-dried sample BRPS-0 exhibits an irregular granular structure, characterized by a lighter overall color and a sparse distribution of particles. Some regions contain larger particles, indicating a degree of roughness. In contrast, BRPS-1 presents a more uniform, powdery appearance with smaller, evenly distributed particles, demonstrating excellent dispersibility. BRPS-2 features a radial structure and a darker light yellow hue. The surface of BRPS-3 displays a fine mesh structure, indicative of high dispersibility and uniformity (Fig. 7).

SEM further elucidates the morphological properties of BRPS. At 500x magnification, BRPS-0 reveals distinct crystalline particles with regular shapes and clear edges, confirming the crystalline state of the polysaccharides. As magnification increases to 10,000x, the details of the particles become more pronounced, showcasing unique geometric shapes and smooth surfaces. Both BRPS-1 and BRPS-2 exhibit irregular fragmentary structures at 500x, however, BRPS-1 has a more uniform surface with noticeable cracks, while BRPS-2 displays a chaotic arrangement of particles. At 10,000x magnification, BRPS-1 reveals a complex surface morphology, covered with numerous round particles of irregular shapes and varying sizes, likely representing aggregates of uncrystallized polysaccharides or other substances. The overall surface is relatively rough, exhibiting distinct textures and undulations, consistent with visual observations [46]. In contrast, BRPS-2 shows a more compact and complex surface structure, with relatively rough particles and pronounced unevenness, indicating strong inter-particle interactions. BRPS-3, at 500x magnification, displays a rough and porous structure composed of irregular aggregates, suggesting the presence of amorphous or partially crystalline components. At 10000x magnification, distinct crystalline particles emerge, exhibiting a more ordered arrangement, primarily in square or rectangular shapes with clear edges. The close packing of these crystalline particles indicates strong interactions among them [47].

3.7.3. Infrared spectroscopy analysis

Infrared spectroscopy identified characteristic polysaccharide absorption peaks at 3500, 2900, 1600, 1400, and 1100 cm^{-1} in BRPS-0, BRPS-1, BRPS-2, and BRPS-3 (Fig. 8). A prominent broad peak observed at 3500, 3400, 3420, and 3400 cm^{-1} is indicative of the abundant hydroxyl groups present in the polysaccharides, reflecting various forms and connections of O-H stretching vibrations [48]. The C-H stretching vibrations are detected at 2930 cm^{-1} across all samples, with a slight variation noted at 2940 cm^{-1} for BRPS-3 [49]. Furthermore, the peaks around 1650, 1620, 1610, and 1650 cm^{-1} are attributed to bound water in the structure. The C-H bending vibrations are represented by peaks at 1400, 1410, 1410, and 1370 cm^{-1}. Additionally, the absorption peaks observed at 1040, 1060, 1060, and 1100 cm^{-1} correspond to C-O glycosidic bond stretching, indicating pyranose rings in the polysaccharide [50]. The characteristic absorptions of C-C stretching vibrations are evident at 590, 575, 590, and 540 cm^{-1}. Notably, a weak peak at 1780 cm^{-1} in the FT-IR spectrum of BRPS-0 may be linked to C=O stretching vibrations of ester bonds [51]. Collectively, the findings confirm that BRPS-0, BRPS-1, BRPS-2, and BRPS-3 exhibit the characteristic absorption features typical of polysaccharides.

3.8. Antioxidant activity of BRPS

The five polysaccharides showed increased DPPH scavenging from 100 to 1000 μg/mL (Fig. 9a). At 1000 μg/mL, the BRPS crude extract reached the highest rate (88.78 %), followed by BRPS-2 (75.53 %), BRPS-0 (75.46 %), BRPS-1 (74.96 %), and BRPS-3 (61.12 %). Correspondingly, the ABTS radical inhibition rates were 98.44 %, 43.55 %, 45.40 %, 50.44 %, and 42.09 %, while the FRAP values were 1.44, 0.22, 0.28, 0.29, and 0.24, respectively (Fig. 9b-c).These findings suggest that the BRPS crude extract possesses the highest radical scavenging capacity, likely due to its elevated polyphenol content. Noted for theirstrong antioxidant effects, polyphenols effectively neutralize free radicals and reduce oxidative stress in cells [52]. Among the purified fractions, BRPS-0 demonstrates relatively stable antioxidant activity due to its small relative molecular weight, which enhances its flexibility, solubility, and bioavailability [53]. Its high content of phenolic compounds and sugars,

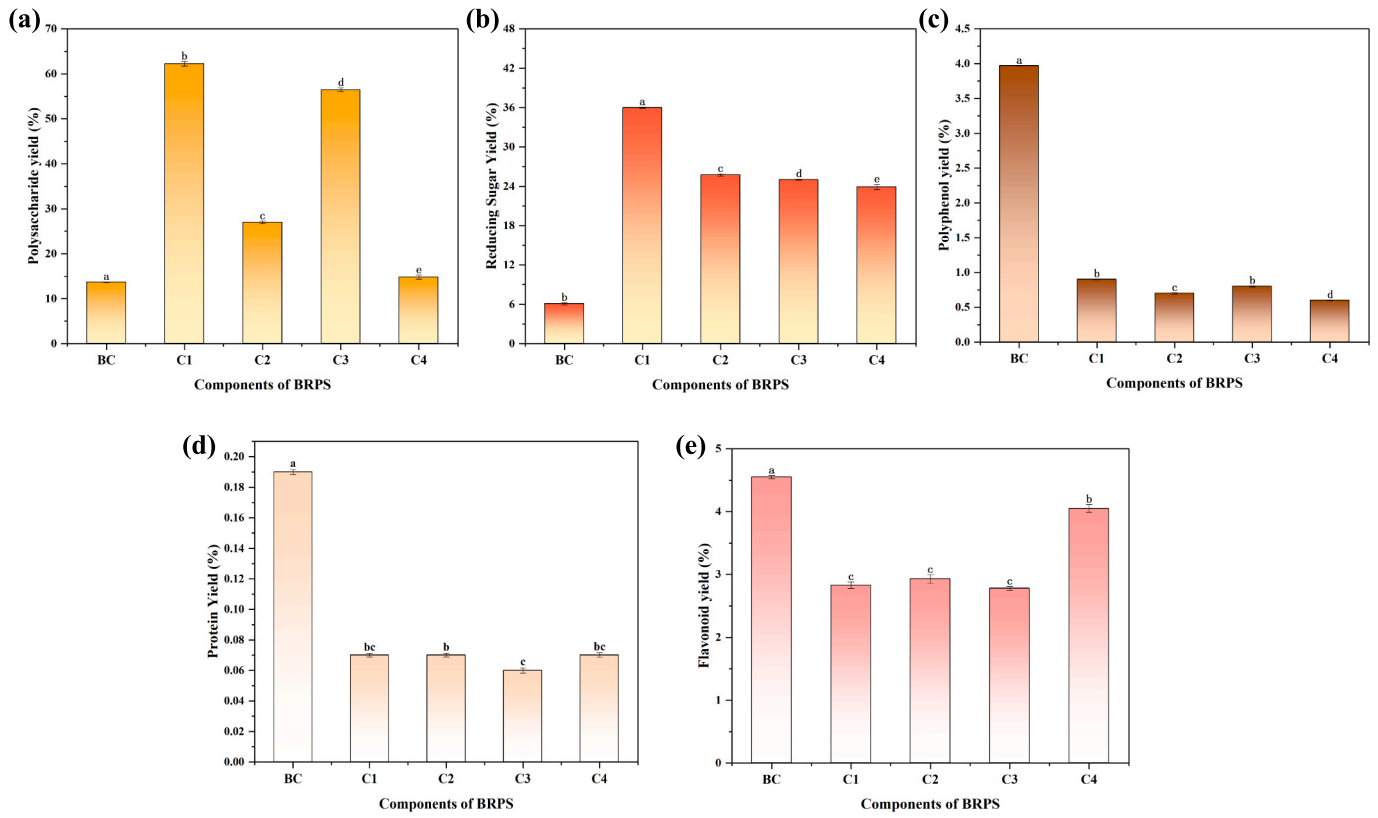

Fig. 6. Physicochemical characteristics of *Boschniakia rossica*'s polysaccharides. (a) polysaccharide yield, (b) reducing sugar yield, (c) polyphenol yield, (d) protein yield, and (e) flavonoid yield (BC: BRPS crude extract, C1: BRPS-0, C2: BRPS-1,C3: BRPS-2, C4: BRPS-3).

Table 3
Molecular weight characteristics of BRPS-0, BRPS-1, BRPS-2 and BRPS-3.

Samples	Number average molecular weight (Mn)	Weight average molecular weight (Mw)	Dispersion coefficient (Mw/Mn)
BRPS-0	1079	1569	1.45
BRPS-1	2007	2815	1.40
BRPS-2	3879	4572	1.18
BRPS-3 (Peak 1)	3957	4871	1.23
BRPS-3 (Peak 2)	890	961	1.08

especially when carbohydrates synergistically interact with polyphenolic substances, can further enhance antioxidant activity [54]. The microstructure of BRPS-0 exhibits high crystallinity and stable molecular arrangement, which allows polysaccharide molecules to be fixed in an ordered structure, thereby enhancing electron delocalization, accelerating free radical capture, and promoting the hydrogen atom transfer (HAT) mechanism, which effectively neutralizes free radicals [55]. Furthermore, the high packing density typically reduces the release rate of active components, resulting in long-lasting antioxidant effects [56]. In contrast, the antioxidant capacity of BRPS-1 is limited by lower sugar content and reduced levels of polyphenols and flavonoids, with surface cracks exacerbating this issue. Although BRPS-2 has higher sugar content, insufficient flavonoid retention and disordered molecular arrangements lead to unstable overall antioxidant activity. Meanwhile, the porous structure of BRPS-3 accelerates the release of active components, resulting in unstable antioxidant effects and overall performance that falls short of BRPS-0.

3.9. Monosaccharide composition and nuclear magnetic resonance of BRPS-0

A preliminary one-dimensional NMR analysis (^{1}H NMR and ^{13}C NMR) was conducted on BRPS-0. The signals in the range of δ 4.5–5.5 ppm represent the anomeric hydrogen signals of the polysaccharide, with α-pyranose resonances typically between δ 4.9–5.3 ppm and β-pyranose resonances between δ 4.4–4.8 ppm (Fig. 10a). Corresponding anomeric carbons appear atδ 90–110 ppm, where α-sugars lie at δ 95–103 ppm and β-sugars above δ 101 ppm (Fig. 10b). Substituted carbons from C-2 to C-5 cluster at δ 65–85 ppm, reflecting glycosylation-induced downfield shifts [57,58].

^{1}H NMR shows multiple anomeric signals in BRPS-0, seven anomeric hydrogen signals were identified at δ 5.40 ppm, δ 5.22 ppm, δ 5.21 ppm, δ 5.19 ppm, δ 5.18 ppm, δ 5.12 ppm, and δ 5.09 ppm, indicating the presence of α-glycosidic residues in BRPS-0. While additional signals at δ 4.4–4.8 ppm suggest β-glycosidic residues. The anomeric carbon signal at δ 95.89 ppm indicates that the sugar residues predominantly exist in the form of pyranose rings [59]. Therefore, it can be preliminarily confirmed that BRPS-0 contains both α and β-configured pyranoses.

Monosaccharide analysis indicates that BRPS-0 is a heteropolysaccharide (galacturonic acid: glucose: galactose:arabinose = 0.352: 3.02: 1.26: 5.37) (Fig. 10c-d). This finding indicates a close relationship between the composition of monosaccharides and their configurations. β-configured pyranoses typically exhibit better solubility and biocompatibility [60], which may suggest higher antioxidant activity in metabolic and functional contexts within biological systems. The higher content of arabinose, galactose, and galacturonic acid contributes to enhancing the polysaccharide's scavenging activity against ABTS and DPPH, consistent with previous antioxidant results [61]. This structural diversity not only imparts different physicochemical properties to the polysaccharide but may also enhance its functionality in biological systems, such as cell recognition and signal transduction [62].

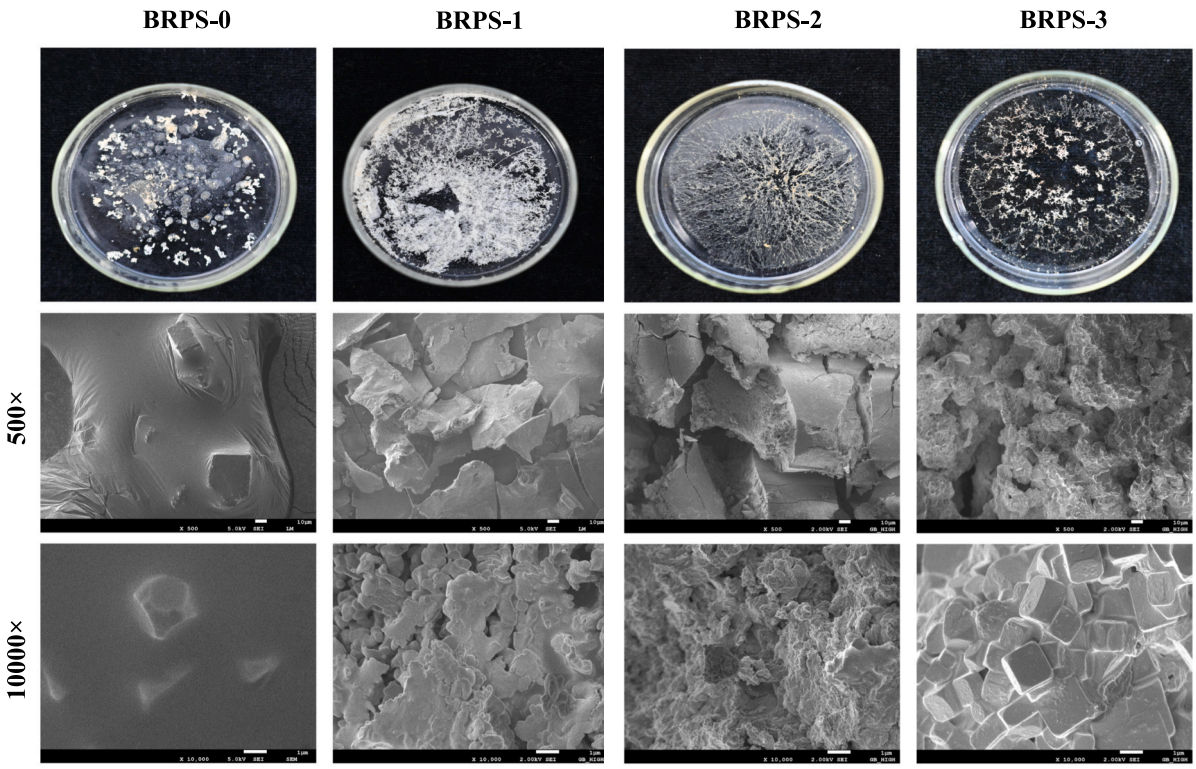

Fig. 7. Scanning electron micrographs (500x, 10000x) of BRPS-0, BRPS-1, BRPS-2 and BRPS-3.

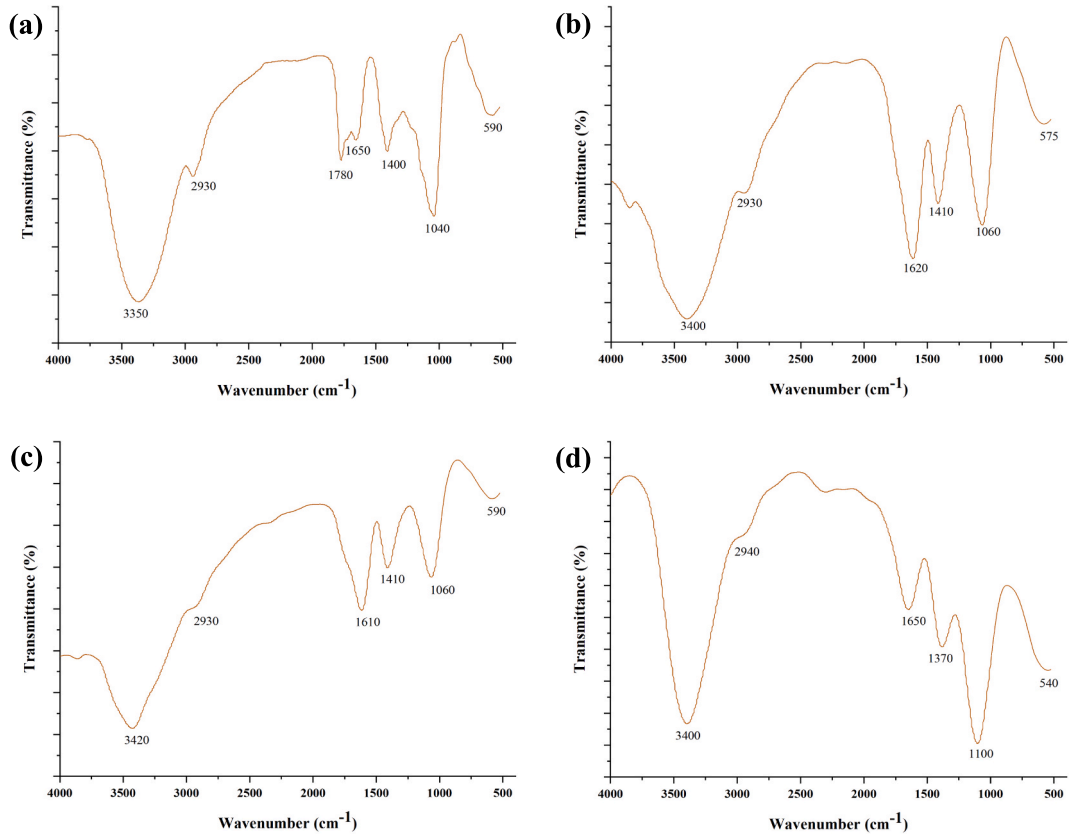

Fig. 8. FT-IR spectrum of BRPS. (a) BRPS-0, (b) BRPS-1, (c) BRPS-2, and (d) BRPS-3.

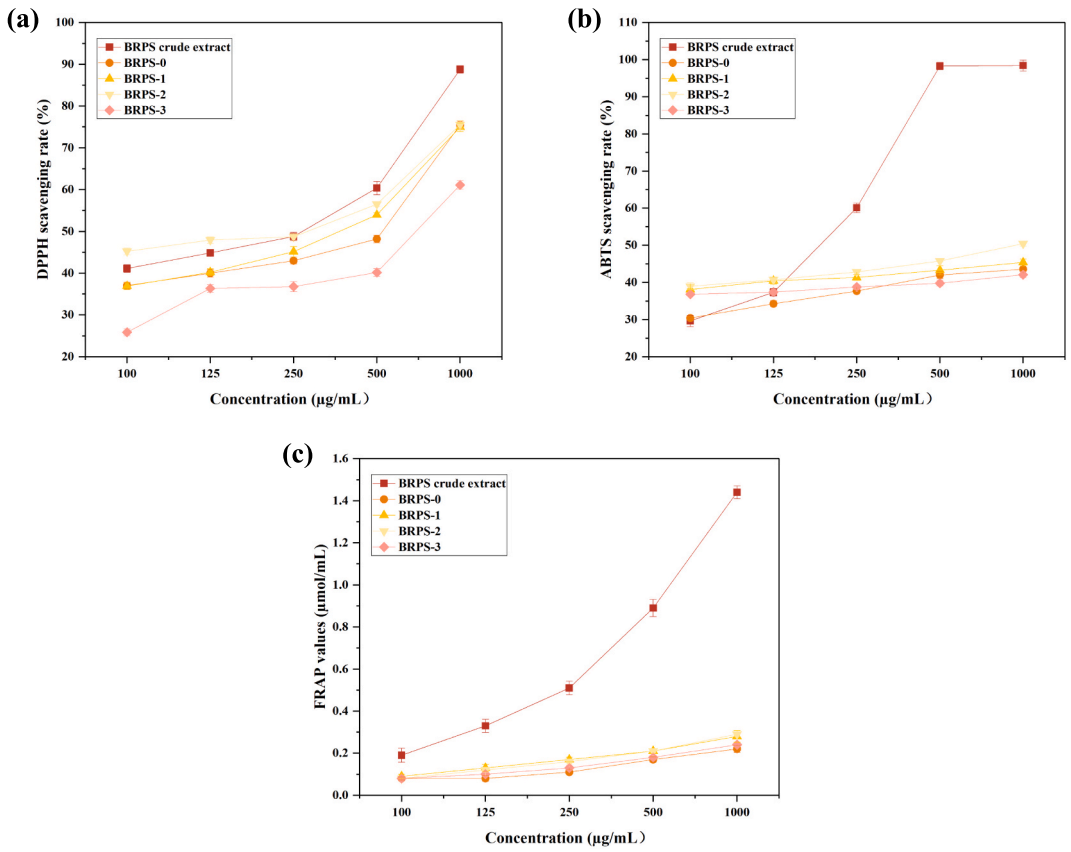

Fig. 9. In vitro antioxidant activity of crude polysaccharides and four purified components from *Boschniakia rossica*. (a) Scavenging ability of polysaccharides on DPPH• free radicals, (b) Scavenging ability of polysaccharides on ABTS• free radicals, (c) Ferric Reducing Antioxidant Potential.

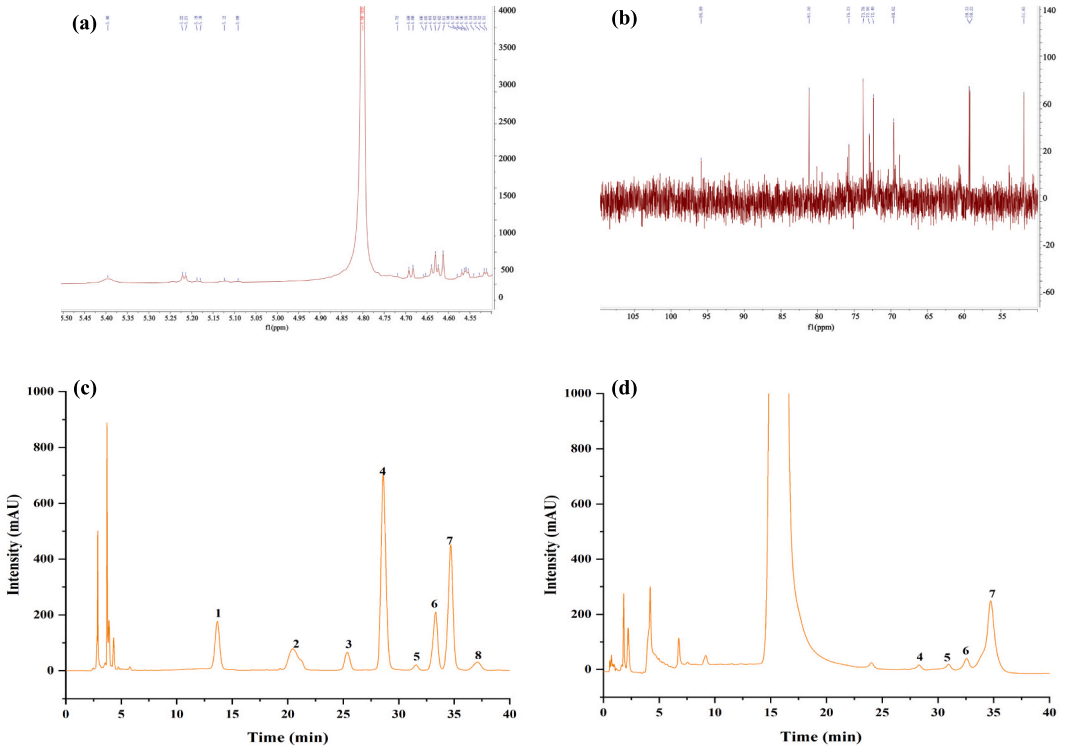

Fig. 10. NMR spectrum and monosaccharide composition analysis of BRPS-0. (a) ^{1}H NMR, (b) ^{13}C NMR, (c) HPLC analysis of mixed standards, and (d) HPLC analysis of the BRPS-0. 1: PMP, 2: Mannose, 3: Glucuronic acid, 4:Galacturonic acid, 5: Glucose, 6: Galactose, 7: Arabinose, and 8: Fucose.

Therefore, the interaction between the composition and configuration of monosaccharides provides an significant structural basis for the biological functions of polysaccharides.

4. Conclusion

This study achieved a 13.67 % yield of crude polysaccharides from *Boschniakia rossica* using UAEE. The four purified polysaccharides showed increased sugar content, while total phenolics and proteins decreased. Relative molecular weight analysis indicated that BRPS-0, BRPS-1, and BRPS-2 had molecular weights of 1569, 2815, and 4572, respectively, demonstrating their homogeneity, while BRPS-3 exhibited high and low molecular weight fractions, reflecting structural complexity. SEM revealed distinct morphologies: BRPS-0 consisted of regular crystalline particles, while BRPS-1 and BRPS-2 appeared as irregular fragments, and BRPS-3 formed cubic crystals. The results indicated that the low molecular weight, high crystallinity, and increased sugar content of BRPS-0 enhanced the stability of its antioxidant bioactivity, with the rising sugar content potentially linked to the synergistic effects of polyphenolic compounds. This underscores the need for further investigation into the interactions between polysaccharides and polyphenols in influencing antioxidant performance. Preliminary structural analysis of BRPS-0 was conducted using NMR and monosaccharide compositional analysis, revealing a close relationship between its microstructure and chemical properties. This study provides important insights into how polysaccharides exert biological activity through their structural characteristics.

Although the antioxidant mechanism of BRPS-0 has been thoroughly investigated, its applications in complex biological systems have yet to be adequately assessed. Furthermore, the lack of long-term studies hinders the understanding of the stability and release characteristics of polysaccharides in vivo. Future research should prioritize examining how structural modifications affect biological activity and anti-tumor effects, while also exploring sugar chain conformations to enhance drug design. Overall, research on the isolation, refinement, structural properties, and biological efficacy of BRPS establishes a vital theoretical foundation for its applications in functional foods and pharmaceuticals.

CRediT authorship contribution statement

Minghui Yang: Writing – review & editing, Writing – original draft, Validation, Methodology, Formal analysis. **Xingfan Li:** Writing – original draft, Validation, Methodology, Formal analysis. **Xinyi Du:** Investigation. **Falin Li:** Investigation. **Tianqi Wang:** Supervision. **Yanyan Gao:** Supervision. **Jia Liu:** Supervision, Methodology. **Xiongfei Luo:** Supervision, Methodology. **Xiaorui Guo:** Supervision, Resources, Funding acquisition. **Zhonghua Tang:** Supervision, Resources, Funding acquisition.

Declaration of competing interest

The authors declare that they have no known competing financial interests or personal relationships that could have appeared to influence the work reported in this paper.

Acknowledgements

This work was supported by the Key R&D Project of Heilongjiang Province (JD22A008), the Seed Industry Innovation Project of Heilongjiang Province (ZQTYB231700002), and the Multidisciplinary Innovation Project of the Heilongjiang Provincial Department of Education (Zxkxt220150001). The authors would like to acknowledge the technical support from the Analysis and Testing Center of Northeast Forestry University.

Appendix A. Supplementary data

Supplementary data to this article can be found online at https://doi.org/10.1016/j.ultsonch.2025.107364.

References

[1] L. Zhang, Y. Zhao, Z.A. Wang, et al., The genus *Boschniakia* in China: An ethnopharmacological and phytochemical review, J. Ethnopharmacol. 194 (2016) 987–1004, https://doi.org/10.1016/j.jep.2016.10.051.
[2] T. Hu, M. Li, X. Zhang, et al., Combination of mass spectrometry analysis and bioinformatic analysis for characterizing anti-inflammation active components from *Boschniakia rossica* and the targets, J. Chromatogr. A 1739 (2025) 465544, https://doi.org/10.1016/j.chroma.2024.465544.
[3] T. Tsuda, A. Sugaya, Y.Z. Liu, et al., Radical scavenger effect of *Boschniakia rossica*, J. Ethnopharmacol. 41 (1994) 85–90, https://doi.org/10.1016/0378-8741(94)90062-0.
[4] Y. Wu, L. Lin, J. Sung, et al., Determination of acteoside in *Cistanche deserticola* and *Boschniakia rossica* and its pharmacokinetics in freely-moving rats using LC–MS/MS, J. Chromatogr. B 844 (2006) 89–95, https://doi.org/10.1016/j.jchromb.2006.07.011.
[5] Z. Wang, C. Lu, C. Wu, et al., Polysaccharide of *Boschniakia rossica* induces apoptosis on laryngeal carcinoma Hep2 cells, Gene 536 (2014) 203–206, https://doi.org/10.1016/j.gene.2013.11.090.
[6] Z. Wang, B. Wu, X. Zhang, et al., Purification of a polysaccharide from *Boschniakia rossica* and its synergistic antitumor effect combined with 5-Fluorouracil, Carbohydr. Polym. 89 (2012) 31–35, https://doi.org/10.1016/j.carbpol.2012.02.024.
[7] J. Chen, W. Ge, P. Wang, et al., Comparison of extraction process, physicochemical properties, and in vitro digestion characteristics of chia seed mucilage polysaccharide, Int. J. Biol. Macromol. 283 (2024) 137739, https://doi.org/10.1016/j.ijbiomac.2024.137739.
[8] W. Chen, X. Ma, W. Jin, et al., Shellfish polysaccharides: A comprehensive review of extraction, purification, structural characterization, and beneficial health effects, Int. J. Biol. Macromol. 279 (2024) 135190, https://doi.org/10.1016/j.ijbiomac.2024.135190.
[9] L. Jiang, K. Zheng, Extraction of mucilage polysaccharides from chia seed by hydrophobic deep eutectic solvents-based three-phase partitioning system: A phase behavior-driven approach, Int. J. Biol. Macromol. 280 (2024) 135913, https://doi.org/10.1016/j.ijbiomac.2024.135913.
[10] T. Lei, Z. Qin, L. Liu, et al., A salt/salt aqueous two-phase system based on pH-switchable deep eutectic solvent for the extraction and separation of mulberry polysaccharides, Food Chem. 462 (2025) 141024, https://doi.org/10.1016/j.foodchem.2024.141024.
[11] M. Dabbour, H. Jiang, B.K. Mintah, et al., Ultrasonic-assisted protein extraction from sunflower meal: Kinetic modeling, functional, and structural traits, Innov. Food Sci. Emerg. Technol. 74 (2021) 102824, https://doi.org/10.1016/j.ifset.2021.102824.
[12] Y.-R. Ma, Y.-Q. Xu, W. Guo, et al., Combined ANFIS and numerical methods to reveal the mass transfer mechanism of ultrasound-enhanced extraction of proteins from millet, Ultrason. Sonochem. 111 (2024) 107153, https://doi.org/10.1016/j.ultsonch.2024.107153.
[13] F. Yeasmin, P. Prasad, J.K. Sahu, Effect of ultrasound on physicochemical, functional and antioxidant properties of red kidney bean (Phaseolus vulgaris L.) proteins extract, Food Bioscience 57 (2024) 103599, https://doi.org/10.1016/j.fbio.2024.103599.
[14] S.S. Nadar, P. Rao, V.K. Rathod, Enzyme assisted extraction of biomolecules as an approach to novel extraction technology: A review, Food Res. Int. 108 (2018) 309–330, https://doi.org/10.1016/j.foodres.2018.03.006.
[15] M.-R. Meini, I. Cabezudo, C.E. Boschetti, et al., Recovery of phenolic antioxidants from Syrah grape pomace through the optimization of an enzymatic extraction process, Food Chem. 283 (2019) 257–264, https://doi.org/10.1016/j.foodchem.2019.01.037.
[16] I.F. Olawuyi, S.R. Kim, D. Hahn, et al., Influences of combined enzyme-ultrasonic extraction on the physicochemical characteristics and properties of okra polysaccharides, Food Hydrocoll. 100 (2020) 105396, https://doi.org/10.1016/j.foodhyd.2019.105396.
[17] S. Wang, Z. Liu, S. Zhao, et al., Effect of combined ultrasonic and enzymatic extraction technique on the quality of noni (Morinda citrifolia L.) juice, Ultrason. Sonochem. 92 (2023) 106231, https://doi.org/10.1016/j.ultsonch.2022.106231.
[18] Y. Yang, Z. Wang, D. Hu, et al., Efficient extraction of pectin from sisal waste by combined enzymatic and ultrasonic process, Food Hydrocoll. 79 (2018) 189–196, https://doi.org/10.1016/j.foodhyd.2017.11.051.
[19] Y. Wang, G. Huang, H. Huang, Ultrasonic/enzymatic extraction, characteristics and comparison of leechee peel polysaccharide, Ultrason. Sonochem. 108 (2024) 106948, https://doi.org/10.1016/j.ultsonch.2024.106948.
[20] N. Cheng, H. Wang, H. Hao, et al., Research progress on polysaccharide components of *Cistanche deserticola* as potential pharmaceutical agents, Eur. J. Med. Chem. 245 (2023) 114892, https://doi.org/10.1016/j.ejmech.2022.114892.
[21] S. Jiang, Y. Cui, B. Wang, et al., Acidic polysaccharides from *Cistanche deserticola* and their effects on the polarization of tumor-associated macrophages, Int. J. Biol. Macromol. 282 (2024) 137207, https://doi.org/10.1016/j.ijbiomac.2024.137207.
[22] Y. Liu, Y. Sheng, G. Yuan, et al., Purification and physicochemical properties of different polysaccharide fractions from the water extract of *Boschniakia rossica* and

their effect on macrophages activation, Int. J. Biol. Macromol. 49 (2011) 1007–1011, https://doi.org/10.1016/j.ijbiomac.2011.08.024.
[23] X. Li, Y. Zhang, J. Wang, et al., Revealing the metabolomics and biometrics underlying phytotoxicity mechanisms for polystyrene nanoplastics and dibutyl phthalate in dandelion (*Taraxacum officinale*), Sci. Total Environ. 905 (2023) 167071, https://doi.org/10.1016/j.scitotenv.2023.167071.
[24] Q.C. Wang, X. Zhao, J.H. Pu, et al., Influences of acidic reaction and hydrolytic conditions on monosaccharide composition analysis of acidic, neutral and basic polysaccharides, Carbohydr. Polym. 143 (2016) 296–300, https://doi.org/10.1016/j.carbpol.2016.02.023.
[25] Q. Chu, S. Xie, H. Wei, et al., Enzyme-assisted ultrasonic extraction of total flavonoids and extraction polysaccharides in residue from *Abelmoschus manihot* (L), Ultrason. Sonochem. 104 (2024) 106815, https://doi.org/10.1016/j.ultsonch.2024.106815.
[26] G. Liu, M. Kamilijiang, A. Abuduwaili, et al., Isolation, structure elucidation, and biological activity of polysaccharides from *Saussurea involucrata*, Int. J. Biol. Macromol. 222 (2022) 154–166, https://doi.org/10.1016/j.ijbiomac.2022.09.137.
[27] A.S.A. Mohammed, M. Naveed, N. Jost, Polysaccharides; classification, chemical properties, and future perspective applications in fields of pharmacology and biological medicine (A review of current applications and upcoming potentialities), J. Polym. Environ. 29 (2021) 2359–2371, https://doi.org/10.1007/s10924-021-02052-2.
[28] T. Niyigaba, D. Liu, J.D. Habimana, The extraction, functionalities and applications of plant polysaccharides in fermented foods: A review, Foods 10 (2021) 3004, https://doi.org/10.3390/foods10123004.
[29] T. Wu, W. Zhu, L. Chen, et al., A review of natural plant extracts in beverages: Extraction process, nutritional function, and safety evaluation, Food Res. Int. 172 (2023) 113185, https://doi.org/10.1016/j.foodres.2023.113185.
[30] B. Zhang, Y. Gao, L. Zhang, et al., The plant cell wall: Biosynthesis, construction, and functions, J. Integr. Plant Biol. 63 (2021) 251–272, https://doi.org/10.1111/jipb.13055.
[31] Z. Rashida, S. Laxman, The pentose phosphate pathway and organization of metabolic networks enabling growth programs, Curr. Opin. Syst. Biol. 28 (2021) 100390, https://doi.org/10.1016/j.coisb.2021.100390.
[32] F. Zulfiqar, N.A. Akram, M. Ashraf, Osmoprotection in plants under abiotic stresses: new insights into a classical phenomenon, Planta 251 (2019) 3, https://doi.org/10.1007/s00425-019-03293-1.
[33] M. Hasanuzzaman, M.M. Alam, A. Rahman, et al., Exogenous proline and glycine betaine mediated upregulation of antioxidant defense and glyoxalase systems provides better protection against salt-induced oxidative stress in two rice (*Oryza sativa* L.) varieties, Biomed Res. Int. 2014 (2014) 757219, https://doi.org/10.1155/2014/757219.
[34] J. Yu, Y. Long, J. Chi, et al., Effects of ethanol concentrations on primary structural and bioactive characteristics of *Dendrobium officinale* polysaccharides, Nutrients 16 (2024) 897, https://doi.org/10.3390/nu16060897.
[35] Z. Tang, G. Huang, H. Huang, Ultrasonic/cellulase-assisted extraction of polysaccharide from *Garcinia mangostana* rinds and its carboxymethylated derivative, Ultrason. Sonochem. 99 (2023) 106571, https://doi.org/10.1016/j.ultsonch.2023.106571.
[36] Y. Wang, Y. Liu, Y. Hu, Optimization of polysaccharides extraction from *Trametes robiniophila* and its antioxidant activities, Carbohydr. Polym. 111 (2014) 324–332, https://doi.org/10.1016/j.carbpol.2014.03.083.
[37] J. Prakash Maran, V. Mekala, S. Manikandan, Modeling and optimization of ultrasound-assisted extraction of polysaccharide from *Cucurbita moschata*, Carbohydr. Polym. 92 (2013) 2018–2026, https://doi.org/10.1016/j.carbpol.2012.11.086.
[38] S. Yang, X. Li, H. Zhang, Ultrasound-assisted extraction and antioxidant activity of polysaccharides from *Tenebrio molitor*, Sci. Rep. 14 (2024) 28526, https://doi.org/10.1038/s41598-024-79482-0.
[39] W. Zhang, W. Duan, G. Huang, et al., Ultrasonic-assisted extraction, analysis and properties of mung bean peel polysaccharide, Ultrason. Sonochem. 98 (2023) 106487, https://doi.org/10.1016/j.ultsonch.2023.106487.
[40] Z. Ying, X. Han, J. Li, Ultrasound-assisted extraction of polysaccharides from mulberry leaves, Food Chem. 127 (2011) 1273–1279, https://doi.org/10.1016/j.foodchem.2011.01.083.
[41] Y. Sun, J. Lu, J. Li, et al., Optimization of ultrasonic-assisted extraction of polyphenol from Areca nut (Areca catechu L.) seeds using response surface methodology and its effects on osteogenic activity, Ultrason. Sonochem. 98 (2023) 106511, https://doi.org/10.1016/j.ultsonch.2023.106511.
[42] Q. Zhao, J.F. Kennedy, X. Wang, et al., Optimization of ultrasonic circulating extraction of polysaccharides from *Asparagus officinalis* using response surface methodology, Int. J. Biol. Macromol. 49 (2011) 181–187, https://doi.org/10.1016/j.ijbiomac.2011.04.012.
[43] T. Ma, X. Sun, C. Tian, et al., Polysaccharide extraction from *Sphallerocarpus gracilis* roots by response surface methodology, Int. J. Biol. Macromol. 88 (2016) 162–170, https://doi.org/10.1016/j.ijbiomac.2016.03.058.
[44] Y. Wang, X. Xiong, G. Huang, Ultrasound-assisted extraction and analysis of *maidenhairtree* polysaccharides, Ultrason. Sonochem. 95 (2023) 106395, https://doi.org/10.1016/j.ultsonch.2023.106395.
[45] M. Puri, D. Sharma, C.J. Barrow, Enzyme-assisted extraction of bioactives from plants, Trends Biotechnology 30 (2012) 37–44, https://doi.org/10.1016/j.tibtech.2011.06.014.
[46] Z. Zhu, J. Chen, Y. Chen, et al., Extraction, structural characterization and antioxidant activity of turmeric polysaccharides, Lwt 154 (2022) 112805, https://doi.org/10.1016/j.lwt.2021.112805.
[47] S. Zhou, G. Huang, Extraction, structure characterization and biological activity of polysaccharide from coconut peel, Chem. Biol. Technol. Agric. 10 (2023) 15, https://doi.org/10.1186/s40538-023-00391-x.
[48] Y. Zhao, F. Nie, W. Liu, et al., Preparation and exploration of anti-tumor activity of *Poria cocos* polysaccharide gold nanorods, Int. J. Biol. Macromol. 280 (2024) 135347, https://doi.org/10.1016/j.ijbiomac.2024.135347.
[49] X. Yang, Y. Gao, M. Reyimu, et al., Structural analysis of *Pleurotus ferulae* polysaccharide and its effects on plant fungal disease and plant growth, Int. J. Biol. Macromol. 282 (2024) 137396, https://doi.org/10.1016/j.ijbiomac.2024.137396.
[50] L. Xiao, J. Hou, P. Chen, et al., Isolation, characterization, and activity of the polysaccharides in *Bulbophyllum kwangtumgense Schltr*, Int. J. Biol. Macromol. 283 (2024) 137382, https://doi.org/10.1016/j.ijbiomac.2024.137382.
[51] H. Hu, Q. Zhao, J. Xie, et al., Polysaccharides from pineapple pomace: new insight into ultrasonic-cellulase synergistic extraction and hypoglycemic activities, Int. J. Biol. Macromol. 121 (2019) 1213–1226, https://doi.org/10.1016/j.ijbiomac.2018.10.054.
[52] F.F. de Araújo, D. de Paulo Farias, I.A. Neri-Numa, et al., Polyphenols and their applications: An approach in food chemistry and innovation potential, Food Chem. 338 (2021) 127535, https://doi.org/10.1016/j.foodchem.2020.127535.
[53] Q. Lee, Z. Xue, Y. Luo, et al., Low molecular weight polysaccharide of *Tremella fuciformis* exhibits stronger antioxidant and immunomodulatory activities than high molecular weight polysaccharide, Int. J. Biol. Macromol. 281 (2024) 136097, https://doi.org/10.1016/j.ijbiomac.2024.136097.
[54] J. Peinado, N. López de Lerma, R.A. Peinado, Synergistic antioxidant interaction between sugars and phenolics from a sweet wine, Eur. Food Res. Technol. 231 (2010) 363–370, https://doi.org/10.1007/s00217-010-1279-6.
[55] N. Zhang, Y. Wu, M. Qiao, et al., Structure–antioxidant activity relationships of dendrocandin analogues determined using density functional theory, Struct. Chem. 33 (2022) 795–805, https://doi.org/10.1007/s11224-022-01895-2.
[56] W. Park, S. Park, K.-Y. Park, et al., Long-term antioxidant metal–organic frameworks, ACS Omega 9 (2024) 21484–21493, https://doi.org/10.1021/acsomega.4c01993.
[57] M.M. de Carvalho, C.F. Ellefsen, A.A. Eltvik, et al., Chemical structure characterization of polysaccharides using diffusion ordered NMR spectroscopy (DOSY), Carbohydr. Polym. 349 (2025) 123021, https://doi.org/10.1016/j.carbpol.2024.123021.
[58] Y. Liu, Y. Ye, X. Hu, et al., Structural characterization and anti-inflammatory activity of a polysaccharide from the lignified okra, Carbohydr. Polym. 265 (2021) 118081, https://doi.org/10.1016/j.carbpol.2021.118081.
[59] L. Tao, Q. Wu, H. Liu, et al., Improved the physicochemical properties and bioactivities of oligosaccharides by degrading self-extracting/commercial ginseng polysaccharides, Int. J. Biol. Macromol. 279 (2024) 135522, https://doi.org/10.1016/j.ijbiomac.2024.135522.
[60] L. Chen, M.D. Ge, Y.J. Zhu, et al., Structure, bioactivity and applications of natural hyperbranched polysaccharides, Carbohydr. Polym. 223 (2019) 115076, https://doi.org/10.1016/j.carbpol.2019.115076.
[61] J. Yi, X. Li, S. Wang, et al., Steam explosion pretreatment of *Achyranthis bidentatae* radix: Modified polysaccharide and its antioxidant activities, Food Chem. 375 (2022) 131746, https://doi.org/10.1016/j.foodchem.2021.131746.
[62] Y. Yu, M. Shen, Q. Song, et al., Biological activities and pharmaceutical applications of polysaccharide from natural resources: A review, Carbohydr. Polym. 183 (2018) 91–101, https://doi.org/10.1016/j.carbpol.2017.12.009.